Acta Crystallographica Section D
**Biological Crystallography**
ISSN 0907-4449

# An ultraviolet fluorescence-based method for identifying and distinguishing protein crystals

**Russell A. Judge,* Kerry Swift and Carlos González**

Abbott Laboratories, 100 Abbott Park Road, Abbott Park, IL 60064, USA

Correspondence e-mail: russell.judge@abbott.com

Received 20 August 2004
Accepted 19 October 2004

Intrinsic ultraviolet fluorescence has been investigated as a rapid non-invasive method for identifying and distinguishing protein crystals. An epi-fluorescence microscope, which provides for excitation and viewing of fluorescence from above the sample, and a straight-through geometry, which provides excitation from above and views fluorescence from underneath the sample, were tested with protein and non-protein crystal samples. In both systems the protein crystals were observed to fluoresce brightly, providing a high contrast against background solution fluorescence, thus enabling protein crystals to be identified and distinguished from non-protein crystals.

## 1. Introduction

Structural biology requires the growth of individual crystals for X-ray diffraction analysis. As the crystallization behavior of a target protein is not usually known beforehand, investigators use screens that contain a wide variety of precipitants (polyethylene glycols of various molecular weights, salts and alcohols), buffers providing a range of solution pH, cofactors and additives. A broad screening exercise can contain hundreds of different solution conditions. Crystal growth is time-dependent, requiring that researchers inspect these crystallization experiments over time. With hundreds of experiments viewed multiple times, the total number of experiments to be viewed can become monumental. When crystallization does occur, crystals may only be observed in a handful of conditions.

To ease the burden of manually identifying crystals among so many unsuccessful experiments, automatic crystal-detection algorithms have been developed. Such methods usually rely on edge detection or contrast to identify crystals (Bern *et al.*, 2004; Cumbaa *et al.*, 2003; Rupp, 2003; Singer & Bilgram, 2004; Spraggon *et al.*, 2002; Wilson, 2002, 2004). However, amorphous precipitates or the drying skin of crystallization drops can also present apparent straight edges, leading to false positives (Cumbaa *et al.*, 2003). Crystals can be obscured by amorphous precipitates and possibly overlooked. To add to the misery of the task, non-protein crystals can also form in the crystallization experiments owing to combination of the precipitants, buffers and additives present in screens together with the components of the protein solution. These non-protein crystals look the same as protein crystals and are usually distinguished by putting the crystal in the X-ray beam. This process can be time-consuming if the crystals are small and require an optimization step to enlarge them sufficiently for X-ray diffraction. To enhance detection techniques it is therefore desirable to increase the contrast between the crystal and the background solution in order to make the

crystal stand out and to distinguish protein from non-protein crystals.

Existing methods of microscopy of materials have limitations in their application to these types of samples. Phase, birefringence, retardance, crossed-polarizer or other contrast methods using visible light and, for example, exploiting the difference in index of refraction between protein crystal and solution may not be conclusive enough alone to allow convenient or rapid scoring of crystallization attempts. Cross-polarization, for example, uses the anisotropic nature of crystalline materials to refract light and produce birefringence (Echalier *et al.*, 2004; Nollert, 2003). Birefringent crystals appear as rainbow-colored objects against a dark background. Crystals with little structural anisotropy may not be birefringent (Bodenstaff *et al.*, 2002): for example, the bacterial cell-division protein FtsZ (Lowe & Amos, 1998). If the isotropic nature of such protein crystals that grow from a given sample is not known before screening, the use of birefringence may result in missed hits. Many organic and inorganic materials present in crystallization screens can also form birefringent crystals that result in false positives.

For spectral information, crystals are generally removed and mounted in instruments for examination (Asanov *et al.*, 2001; Bourgeois *et al.*, 2002). For high throughput, an *in situ* method is preferable. Absorbance or transmitted light microscopy in the ultraviolet may be difficult in the plastic plates that are typically used as crystal-growth containers (DeLucas & Bray, 2004). Chemical modification of a protein prior to crystallization (such as attaching a fluorescent probe; Ikkai & Shimada, 2002; Sumida *et al.*, 2001) in order to visualize the crystals more easily when they form is usually undesirable because of the risk of denaturing the protein or altering its biochemical (*e.g.* compound-binding) properties in subtle or major ways. The crystallization behavior of the protein may also be altered unpredictably. In order to recognize protein crystals, dyes that absorb into or stain protein specifically can be added to a crystallization well during or after crystal formation (Izit Crystal Dye, Hampton Research, Aliso Viejo, CA, USA; Cosenza *et al.*, 2003). However, such a process can modify crystals substantially and can alter or abrogate the binding of any drug-like compound under study and is thus limited to cases where the crystals need not be harvested.

In view of the above, a definite need exists for fast non-invasive methods that allow for the precise visualization of protein crystals in such a way that they can be distinguished from other materials. To this end, the use of intrinsic protein fluorescence has been investigated.

## 2. Experimental methods

### 2.1. Native ultraviolet fluorescence of proteins

For proteins the amino acid tryptophan absorbs ultraviolet light in the range 260–320 nm, with peak absorbance at 280 nm. Tyrosine and phenylalanine also absorb in this range, but not as strongly as tryptophan. Tryptophan fluorescence is detected from approximately 300 to 450 nm, with peak emission at 340–360 nm (Lakowicz, 1999; Permyakov, 1993). An additional strong absorption band at higher energy for tryptophan and tyrosine may allow luminescence excitation at lower wavelengths (*e.g.* <260 nm); however, as buffer constituents or crystallization-plate materials might cause significant interference, thus reducing contrast, the longer wavelengths were used.

### 2.2. Background fluorescence

Six 96-well screening grids [Crystal Screen and Index (Hampton Research, Aliso Viejo, CA, USA), Cryo Bloc and Wizard (Emerald Biostructures Products, Bainbridge Island, WA, USA) and Jena Bioscience high-throughput I and II (Jena, Germany)] were tested for background fluorescence. These screens contain components typical of commercial screens. The solutions were excited at 280 nm and fluorescence was detected at 350 nm using a quartz plate and plate reader. Fig. 1 illustrates the result for Crystal Screen. The solutions only fluoresce to a limited degree, producing less than 30% background with respect to the level expected for typical solution protein fluorescence. For example, lysozyme at 2 mg ml$^{-1}$ in 0.1 *M* sodium acetate buffer pH 4.65 exhibited fluorescence of 4800 relative fluorescence units (RFUs). In the screens tested, the components with the highest background fluorescence were PEG MMEs (polyethylene glycol monomethyl ethers; Brzozowski & Tolley, 1994). Again, this fluorescence is still small compared with that of protein in crystals.

In the use of crystallization plates, covers made of glass or plastic are used to prevent evaporation. These thin sheets or cover slips can pass the excitation light to a sufficient degree to allow this method to work successfully. Plastics used in the

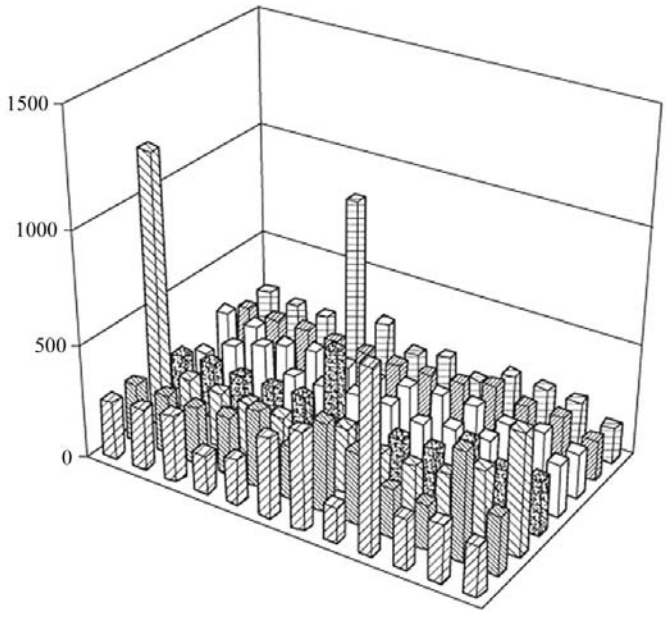


**Figure 1**
Background fluorescence (given as relative fluorescence units, RFU) from solutions in Crystal Screen (Hampton Research, Aliso Viejo, CA, USA). $\lambda_{ex}$ = 280 nm; $\lambda_{em}$ = 350 nm. For the 96-well block, A1 is in the top-left corner and H12 is in the bottom-right corner.

sample-container floor or its frame were also found to transmit fluorescence to a sufficient degree to permit them to be used for detecting protein fluorescence.

### 2.3. Ultraviolet fluorescence imaging

Biological fluorescence microscopy refers today mostly to work with excitation in the visible range or near-ultraviolet range [commonly at 365 nm (McCrone *et al.*, 1978) or 351 nm for confocal UV laser scanning microscopy] of the electromagnetic spectrum. The process often involves the use of purpose-specific dyes or visibly fluorescent proteins (*e.g.* green fluorescent protein; GFP) incorporated or conjugated to proteins or other molecules in some way, rather than the intrinsic ultraviolet-excited fluorescence of proteins, nucleic acids or other common biological constituents (Tan *et al.*, 1995). For the wavelengths used for exciting intrinsic fluorescence, the glass or antireflection coating used in common objective lenses or other focusing lenses is unsuitable. In fact, most commercially available compound microscopes for fluorescent biological samples contain multiple antireflection-coated glass elements and do not allow excitation in this range of ultraviolet wavelengths (<351 nm). To work at these wavelengths, ultraviolet-transmitting lenses from fused silica ('quartz') are required. In our studies, systems with an epi-fluorescence microscope and a straight-through geometry were tested.

**2.3.1. Epi-fluorescence**. The system used to study epi-fluorescence is illustrated in Fig. 2. In this system the excitation light, a 20 nm band centered at 280 nm, is focused down through the ultraviolet microscope objective. The fluorescence light from the sample was collected in a 40 nm band centered at 360 nm through the same microscope objective and detected using an ultraviolet-sensitive video camera. Visible (side illumination) and ultraviolet fluorescent images were acquired using this instrument.

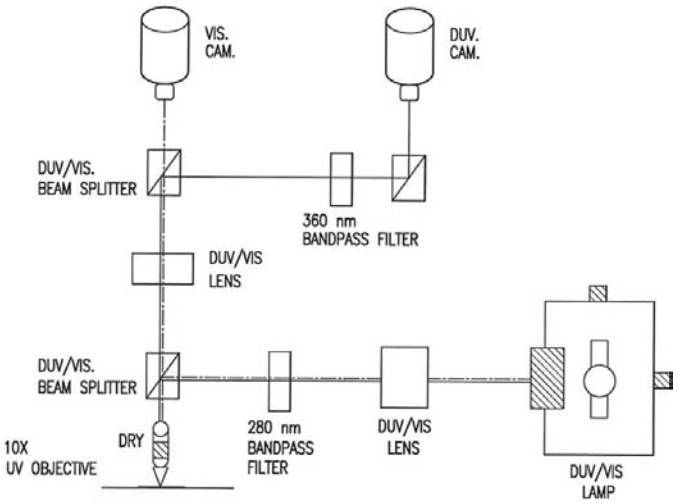


**Figure 2**
A block diagram of the ultraviolet epi-fluorescence microscope. This configuration provides for excitation and viewing of fluorescence from above the sample.

**2.3.2. Straight-through geometry**. The straight-through geometry imaging system was constructed as illustrated in Fig. 3. An ultraviolet-light source (MAX HP; Lightwave Energy Systems Co., Torrance, CA, USA) is coupled into a 5 mm quartz light guide and focused using an *f*/100 UV DCX lens (Edmund Industrial Optics, Barrington, NJ, USA). The output beam is filtered and reflected using a Dichroic Mirror (P/N: N3463 HR@266 nm; US Laser Corporation, Wyckoff, NJ, USA) through two 280 nm bandpass filters (S-P Corion Filter, G25-280-F; Spectra-Physics Franklin, MA, USA) and is finally focused onto the sample solution using a 10× UVB objective (Optics For Research, Verona, NJ, USA). The diameter of the 280 nm light spot is adjusted to fit the cross-section of the sample volume being interrogated. The sample is imaged at 180° to the excitation source through the sample plate using a 10× Plan objective (WD 10.5 mm; Modulation Optics Inc., Greenvale, NY, USA) attached to an integrating CCD camera (ORCA ER 1394 Cooled CCD; Hamamatsu, Bridgewater, NJ, USA) and controlled through software (Simple PCI; Compix Inc., Cranberry Township, PA, USA). The integration time and gain on the camera is adjusted to maximize the contrast of the emission signal at 360 nm. Since the imaging objective had a cutoff wavelength at 330 nm, additional filtering was not used before the CCD. In the case where a UVB objective was used on the imaging side of the system, a 360 nm bandpass filter (P/N: S-P Corion Filter, XMS-360-F; Spectra-Physics, Franklin, MA, USA) was used before the CCD to select fluorescence emission and block excitation light. Ultraviolet fluorescent images were acquired using this instrument. For excitation at 280 nm, the illumination power was 10 µW at the sample and integration times were several seconds. Faster acquisition times can be expected with a brighter light source. Visible-light images were acquired using

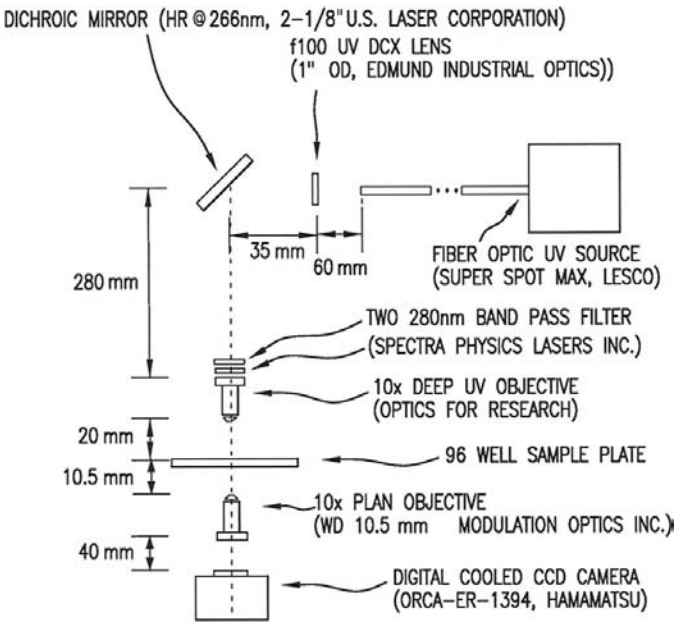


**Figure 3**
The straight-through optical configuration of an ultraviolet fluorescence microscope. In this configuration, the sample is excited from above and the fluorescence emission is viewed from beneath.

an Olympus stereomicroscope Model SZX12 and an Olympus Model DP12 CCD camera (Olympus, Melville, NY, USA).

### 2.4. Crystallization samples

**2.4.1. Glucose isomerase**. Glucose isomerase was obtained from Hampton Research (Aliso Viejo, CA, USA) and dialyzed against distilled water before use. For the experiments using epi-fluorescence, crystals were grown with 10 mg ml$^{-1}$ glucose isomerase in water mixed in a 1:1 ratio with 0.9–2.9 *M* ammonium sulfate and 0.1 *M* HEPES pH 7.7 at 296 K in 24-well Linbro plates (Hampton Research, Aliso Viejo, CA, USA) by the hanging-drop method. Quartz cover slips (Ted Pella Inc., Redding, CA, USA) were used to suspend the drop over the reservoir solution.

For the crystals tested with the straight-through geometry, crystals were grown by vapor diffusion in sitting drops in a 96-well plate (CrystalQuick plate, round-bottom well; Greiner Bio-one Inc., Longwood, FL, USA) covered with ClearSeal film (Hampton Research, Aliso Viejo, CA, USA). Crystals were grown at 296 K using 18 mg ml$^{-1}$ glucose isomerase in (i) 1.6 *M* ammonium sulfate and 0.1 *M* Bicine pH 9.0, (ii) 15% ethanol, 0.1 *M* HEPES pH 7.5 and 0.2 *M* magnesium chloride and (iii) 30% MPD, 0.1 *M* sodium cacodylate pH 6.5 and 0.2 *M* magnesium acetate.

**2.4.2. Chicken egg-white lysozyme**. Lysozyme was purchased from Seikagaku. For epi-fluorescence, crystals were grown by the batch method at room temperature from 100 m*M* sodium acetate buffer pH 4.5 and a 50 mg ml$^{-1}$ solution of protein mixed with an equal volume of 10%(*w*/*v*) NaCl in the same buffer. A reservoir solution containing the same precipitant concentration as the resulting drop [5%(*w*/*v*) salt, same buffer] was used to maintain the composition of the drop over time. The plate format was a 96-well plate (CrystalQuick plate, round-bottom well; Greiner Bio-one Inc., Longwood, FL, USA) covered with ClearSeal film (Hampton Research, Aliso Viejo, CA, USA).

**2.4.3. Salt crystals**. Salt crystals (confirmed by X-ray diffraction analysis, data not shown) were grown using 20 mg ml$^{-1}$ lysozyme in 50 m*M* Tris, 100 m*M* ammonium sulfate, 10% glycerol, 1 m*M* DTT, 1 m*M* magnesium acetate and 1 m*M* sodium azide pH 7.4 mixed in a vapor-diffusion crystallization in a 1:1 ratio with 40% polyethylene glycol 300, 0.2 *M* calcium acetate and 0.1 *M* cacodylate pH 6.5 and equilibrated against a 100 µl reservoir containing 40% polyethylene glycol 300, 0.2 *M* calcium acetate and 0.1 *M* cacodylate pH 6.5. The crystals were grown at 290 K over a period of a few days. For the straight-through geometry, in order to test the ability to distinguish protein from salt crystals, the salt crystals were transferred using a nylon-fiber loop to a 96-well plate with glucose isomerase crystals grown from 30% MPD, 0.1 *M* sodium cacodylate pH 6.5 and 0.2 *M* magnesium acetate.

**2.4.4. Human protein tyrosine phosphatase 1B (PTP1B)**. Human protein tyrosine phosphatase 1B crystals were grown according to the method of Puius *et al.* (1997) (as modified by Szczepankiewicz *et al.*, 2003). In summary, crystals were grown at 277 K by vapor diffusion using 3–4 mg ml$^{-1}$ protein with 2–4 m*M* DTT in 10 m*M* Tris–HCl pH 7.5 and 25 m*M* NaCl mixed in a 1:1 ratio with 0.1 *M* HEPES pH 7.0–7.5, 0.2 *M* magnesium acetate and 12–14% polyethylene glycol 8000 and equilibrated over 1 ml of 0.1 *M* HEPES pH 7.0–7.5, 0.2 *M* magnesium acetate and 12–14% polyethylene glycol 8000.

In this case, the crystals were grown in a Linbro plate using the hanging-drop method. For imaging, the crystals were transferred to a 96-well vapor-diffusion plate with ClearSeal film covering the samples.

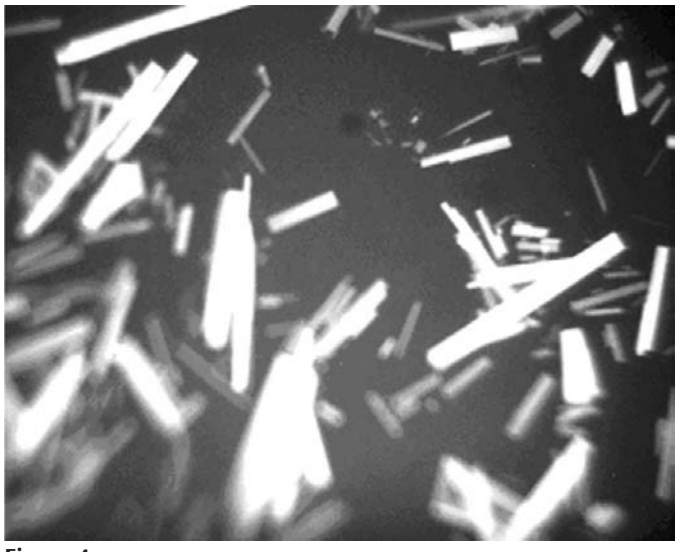

**Figure 4**
Glucose isomerase crystals imaged by ultraviolet fluorescence using the epi-fluorescence geometry. The crystals are in a hanging drop on a quartz cover slip in a Linbro plate.

## 3. Results

### 3.1. Epi-fluorescence

Glucose isomerase crystals are seen to fluoresce brightly in Fig. 4. The bright rod-shaped objects are the protein crystals and the image shows high contrast. These crystals are 100–

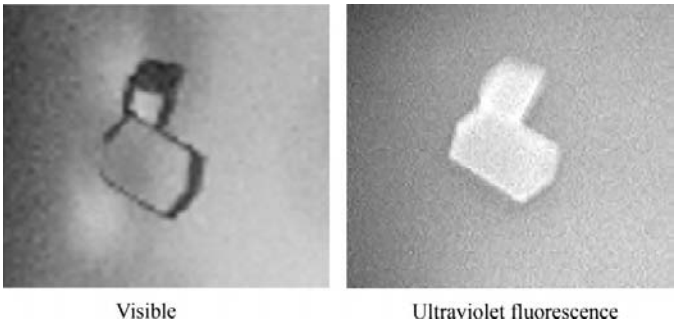


**Figure 5**
Crystals of chicken egg-white lysozyme viewed with visible light (for comparison) and with intrinsic ultraviolet-excited fluorescence using the epi-fluorescence geometry. These crystals are contained in a 96-well sitting-drop plate covered with ClearSeal film. As can be seen, the film presents no significant obstacle for the excitation and collection of the fluorescence emission.

**Table 1**
Tryptophan composition of proteins imaged with ultraviolet fluorescence relative to typical protein tryptophan composition.

| Protein | Tryptophan residues (%) |
|---|---|
| Chicken egg-white lysozyme | 4.7 |
| Glucose isomerase | 1.6 |
| PTP1B | 1.9 |
| Typical protein composition | 1.4 |

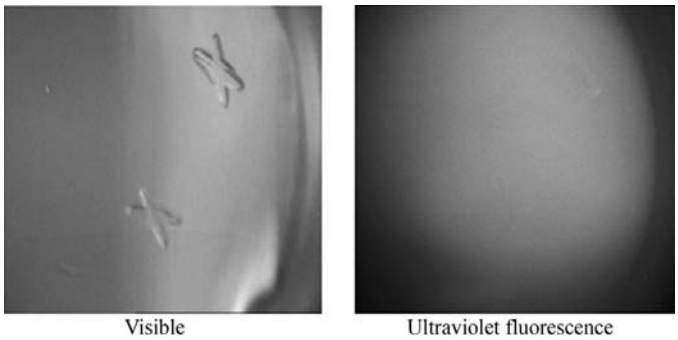


**Figure 6**
Crystals of salt, viewed with visible light, but disappearing under the conditions and with the same setup used for viewing intrinsic ultraviolet-excited fluorescence of protein crystals.

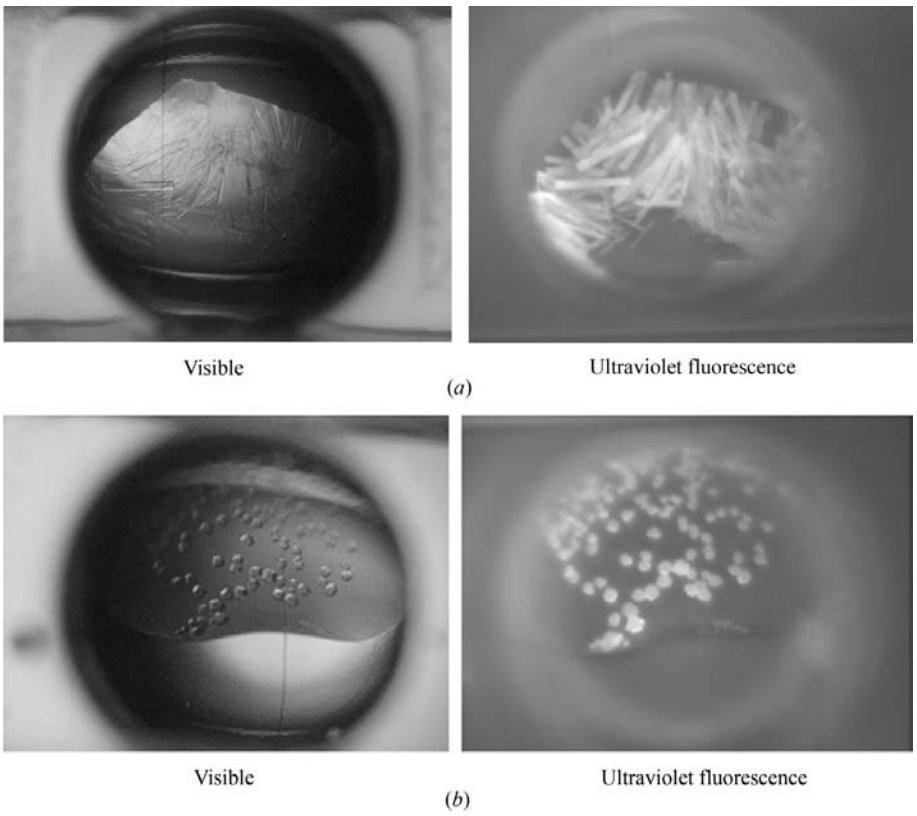


**Figure 7**
Glucose isomerase crystals viewed with visible light and visualized by ultraviolet fluorescence imaged in the straight-through geometry. The crystals are in 96-well plates covered with ClearSeal film and were grown in (*a*) 1.6 *M* ammonium sulfate, 0.1 *M* Bicine pH 9.0, 18 mg ml$^{-1}$ glucose isomerase at 296 K and (*b*) 15% ethanol, 0.1 *M* HEPES pH 7.5, 0.2 *M* magnesium chloride, 18 mg ml$^{-1}$ glucose isomerase at 296 K.

200 µm in length and are clearly seen against the solution still containing some dissolved protein. Variations in brightness from crystal to crystal arise owing to the different depth positions relative to the focal plane of the objective lens and perhaps also to crystal-orientation effects. The epi-fluorescent system works well for this Linbro hanging-drop format, where the required working distance and well contents would impede fluorescence detection in the straight-through geometry. Quartz cover slips provide maximum visibility. Glass cover slips can be used, but the fluorescence is reduced. Interestingly, these crystals were determined to be isotropic in that they show no birefringence with visible light. These particular crystals would therefore be missed in birefringent images.

Lysozyme crystals also brightly fluoresce, as shown in Fig. 5. In this instance, the visible-light image was obtained with an Olympus Model SZX12 stereomicroscope and an Olympus Model DP12 CCD camera. Background fluorescence from the lysozyme in solution is also visible, but is less intense than that of the crystals, probably because of the higher protein concentration in the crystals.

The salt crystals clearly do not fluoresce (Fig. 6) and are not distinguishable in the fluorescent image. The effect is because of the lack of fluorescence of the sample and not because of the ClearSeal film cover over the 96-well plate, as the film presented no problem in the imaging of fluorescent lysozyme crystals.

### 3.2. Straight-through geometry

Two different crystal forms of glucose isomerase are shown to fluoresce brightly in the straight-through geometry (Fig. 7). In the 96-well plates the well is about 2 mm across. The protein-solution droplet had a volume of 1 µl and because it does not fill the well its boundary was visible. Human protein tyrosine phosphatase 1B crystals also fluoresce brightly in this configuration (Fig. 8). In these examples, the plate material below does not pose a significant attenuation to the fluorescent emission passing through it. Salt crystals are also clearly distinguished from protein crystals in this configuration, as illustrated in Fig. 9.

## 4. Discussion

This study demonstrates that intrinsic fluorescence can be used to identify protein crystals. The crystals fluoresce brightly, providing a high contrast against background solution fluorescence. While lysozyme (Canfield, 1963) has a high percentage of tryptophan, glucose isomerase (Carrell *et al.*, 1989)

and PTP1B (Puius *et al.*, 1997) have a percentage of tryptophan residues typical of most proteins (Voet & Voet, 1995) (Table 1), illustrating that the technique should find wide application.

In the limited samples given, the technique also enables protein crystals to be distinguished from non-protein crystals (as would be predicted from their chemical composition). Interestingly, although the protein crystals are clearly brighter than the salt crystal in the straight-through geometry (Fig. 9), the salt crystals exhibit a faint visibility compared with the epi-fluorescence system, where the salt crystals effectively disappear (Fig. 6). This effect is most likely to be a consequence of scattering of the incident excitation light. In the epi-fluorescence geometry, it is necessary to block back-scatter or reflection of the excitation light from the salt crystals; however, back-scatter and reflection will be small compared with the forward scatter and transmission of the excitation light in the straight-through geometry. While the glass objective in the straight-through geometry acts as a filter, there is simply more excitation light to deal with at the camera than there is in the epi-fluorescence geometry. Additional filters may reduce the stray excitation light, but could also attenuate the fluorescent signal. One other possible contribution is that the salt crystal in Fig. 9 may also be reflecting or scattering genuine fluorescence from the nearby protein crystals.

To help further distinguish protein crystals, the brightness of the pixels in the ultraviolet fluorescent images can be determined using imaging-software applications (Adobe Photoshop; Adobe Systems Inc., San Jose, CA, USA), where the brightness of a pixel is assigned a number between 0 and 255 (where 0 is black and 255 is white). The protein crystals in this study are at least 30 units brighter than the background fluorescence adjacent to the crystal, with many exhibiting a difference of 60 or more units. The difference in brightness between the salt crystal in Fig. 9 and the adjacent background fluorescence is less than 30 units.

Ultraviolet fluorescent imaging can be applied to typical crystallization-plate formats (96-well plates and Linbro plates), as the well covers and the plates themselves do not significantly block the fluorescence of the sample. Both geometries can be used with 96-well plates and could be adapted for high-throughput viewing. The epi-fluorescence system is better suited than the straight-through geometry for Linbro plate crystallization formats. In this instance the use of quartz cover slips is preferred. In both fluorescent microscope configurations, the dose of excitation radiation (exposure times) can be controlled. While it was not observed in this study, over-exposure could lead to photobleaching and loss of fluorescence of the sample. However, this effect may also provide a means of confirming genuine fluorescence specific to the desired crystal. Some eventual fading of fluorescence is expected, but accidental pick-up of reflections or other stray light should remain relatively constant. The effect of photobleaching on the structure of the tryptophan in the resulting X-ray diffraction analysis of the crystals so exposed is yet to be determined.

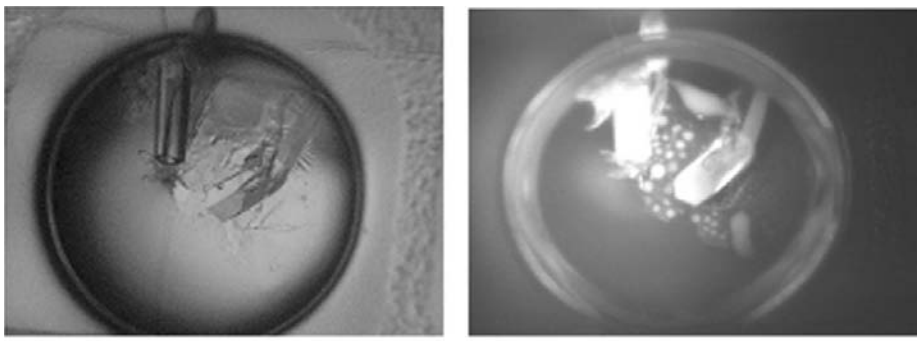


**Figure 8**
Human protein tyrosine phosphatase 1B (PTP1B) crystals viewed with visible light and intrinsic ultraviolet-excited fluorescence. The crystals are in a 96-well plate covered with ClearSeal film viewed with the straight-through geometry.

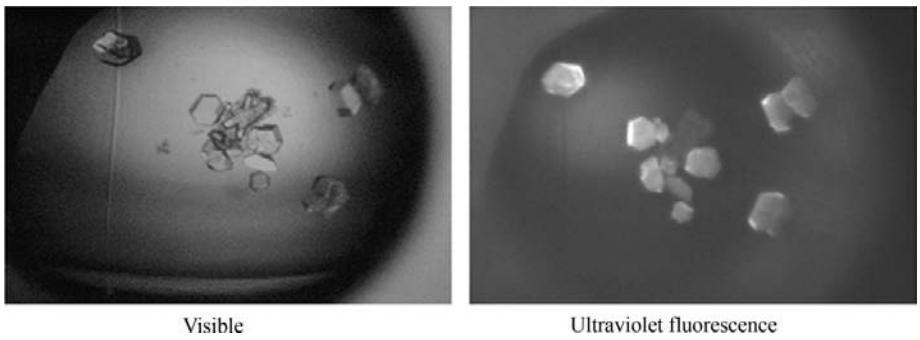


**Figure 9**
Crystals of salt (X-shaped) together with crystals of glucose isomerase (grown by vapor diffusion, 18 mg ml$^{-1}$ protein, 30% MPD, 0.1 *M* sodium cacodylate pH 6.5, 0.2 *M* magnesium acetate) viewed with visible light and distinguished from each other by intrinsic ultraviolet-excited fluorescence. The crystals are in a 96-well plate covered with ClearSeal film viewed with the straight-through geometry. The slight movement of the crystals between the two images arose owing to the transportation of the plate between the visible-light stereomicroscope and the ultraviolet fluorescent straight-through geometry system.

As well as detecting protein crystals by their fluorescence, the technique could also be used to identify whether ligands soaked into the crystals have bound to the protein. Indications of binding could be observed owing to increased fluorescence from the ligand if it is intrinsically fluorescent or decreased fluorescence if the tryptophan fluorescence is reduced or quenched on binding. This is the subject of future work.

## 5. Conclusions

Intrinsic fluorescence can be used to identify and distinguish protein crystals in typical crystallization-plate formats. Specifically designed fluorescence

microscopes provide a fast and non-invasive approach that is well suited to high-throughput crystallography.

The authors acknowledge Korima Inc., Carson, CA, USA for the use of the TnP Instruments epi-fluorescence microscope used in this study. Jeffrey Pan is thanked for useful discussions and suggestions in the development of the straight-through geometry system.

## References

Asanov, A. N., McDonald, H. M., Oldham, P. B., Jedrzejas, M. J. & Wilson, W. W. (2001). *J. Cryst. Growth*, **232**, 603–609.
Bern, M., Goldberg, D., Stevens, R. C. & Kuhn, P. (2004). *J. Appl. Cryst.* **37**, 279–287.
Bodenstaff, E. R., Hoedemaeker, F. J., Kuil, M. E., de Vrind, H. P. & Abrahams, J. P. (2002). *Acta Cryst.* D**58**, 1901–1906.
Bourgeois, D., Vernede, X., Adam, V., Fioravanti, E. & Ursby, T. (2002). *J. Appl. Cryst.* **35**, 319–326.
Brzozowski, A. M. & Tolley, S. P. (1994). *Acta Cryst.* D**50**, 466–468.
Canfield, R. E. (1963). *J. Biol. Chem.* **238**, 2698–2707.
Carrell, H. L., Glusker, J. P., Burger, V., Manfre, F., Tritsch, D. & Biellmann, J. F. (1989). *Proc. Natl Acad. Sci. USA*, **86**, 4440–4444.
Cosenza, L., Bray, T. L., DeLucas, L. J., Gester, T. & Hamrick, D. T. (2003). *Use of Dye to Distinguish Salt and Protein Crystals Under Microcrystallization Conditions.* WO 2003012430. University of Alabama Birmingham Research Foundation, USA.
Cumbaa, C. A., Lauricella, A., Fehrman, N., Veatch, C., Collins, R., Luft, J., DeTitta, G. & Jurisica, I. (2003). *Acta Cryst.* D**59**, 1619–1627.
DeLucas, L. J. & Bray, T. L. (2004). *Method for Distinguishing Between Biomolecule and Non-biomolecule Crystals.* WO 2004/005898 A1. University of Alabama Birmingham Research Foundation, USA.
Echalier, A., Glazer, R. L., Fülöp, V. & Geday, M. A. (2004). *Acta Cryst.* D**60**, 696–702.
Ikkai, T. & Shimada, K. (2002). *J. Fluorescence*, **12**, 167–171.
Lakowicz, J. R. (1999). *Principles of Fluorescence Spectroscopy*, 2nd ed. New York: Kluwer Academic/Plenum Publishers.
Lowe, J. & Amos, L. A. (1998). *Nature* (*London*), **391**, 203–206.
McCrone, W. C., McCrone, L. B. & Delly, J. G. (1978). *Polarized Light Microscopy.* Ann Arbor, MI, USA: Ann Arbor Science.
Nollert, P. (2003). *J. Appl. Cryst.* **36**, 1295–1296.
Permyakov, E. A. (1993). *Luminescent Spectroscopy of Proteins.* Boca Raton, FL, USA: CRC Press.
Puius, Y. A., Zhao, Y., Sullivan, M., Lawrence, D. S., Almo, S. C. & Zhang, Z. Y. (1997). *Proc. Natl Acad. Sci. USA*, **94**, 13420–13425.
Rupp, B. (2003). *Acc. Chem. Res.* **36**, 173–181.
Singer, H. M. & Bilgram, J. H. (2004). *J. Cryst. Growth*, **261**, 122–134.
Spraggon, G., Lesley, S. A., Kreusch, A. & Priestle, J. P. (2002). *Acta Cryst.* D**58**, 1915–1923.
Sumida, J. P., Forsythe, E. L. & Pusey, M. L. (2001). *J. Cryst. Growth*, **232**, 308–316.
Szczepankiewicz, B. G., Liu, G., Hajduk, P. J., Abad-Zapatero, C., Pei, Z., Xin, Z., Lubben, T. H., Trevillyan, J. M., Stashko, M. A., Ballaron, S. J., Liang, H., Huang, F., Hutchins, C. W., Fesik, S. W. & Jirousek, M. R. (2003). *J. Am. Chem. Soc.* **125**, 4087–4096.
Tan, W. H., Parpura, V., Haydon, P. G. & Yeung, E. S. (1995). *Anal. Chem.* **67**, 2575–2579.
Voet, D. & Voet, J. G. (1995). *Biochemistry*, 2nd ed. New York: John Wiley & Sons.
Wilson, J. (2002). *Acta Cryst.* D**58**, 1907–1914.
Wilson, J. (2004). *Crystallogr. Rev.* **10**, 73–84.